Previous Page

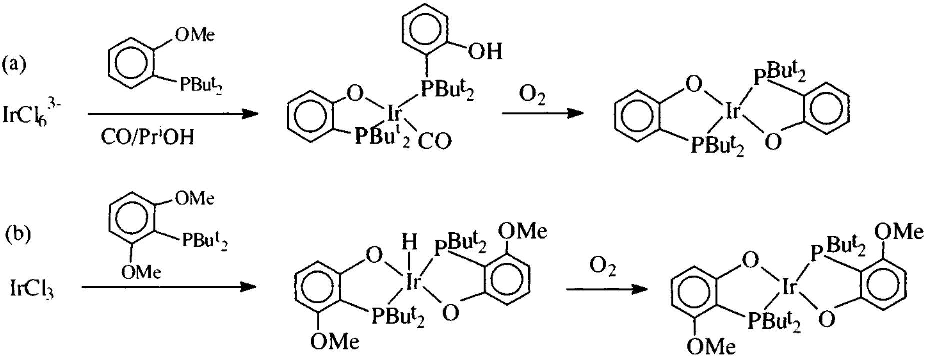

Figure 2.83 Syntheses of iridium(II) phosphine complexes.

2.12 Iridium(II) complexes

The iridium(II) complexes are rarer that those of rhodium(II). Iridium does not seem to form carboxylates $Ir_2(O_2CR)_4$ with the 'lantern' structure; complexes analogous to *trans*-$RhX_2(PR_3)_2$ are not formed with bulky tertiary phosphines, probably because the greater strength of Ir–H bonds leads to $IrHX_2(PR_3)_2$.

The best characterized complexes [146] are prepared as shown in Figure 2.83. In synthesis (a) the first step involves demethylation of both ligands; only one phosphine chelates, demonstrating the stability of square planar d^8 iridium(I); on oxidation, the CO is displaced (as CO_2) and both ligands chelate.

In synthesis (b), the initial product is a 5-coordinate (sp) iridium(III) hydride complex, which is rapidly oxidized in solution to the planar iridium(II) complex. Both of the compounds are paramagnetic with one unpaired electron, as expected for square planar d^7 complexes.

The square planar ion $[Ir(C_6Cl_5)_4]^{2-}$ also contains iridium(II) [147].

2.13 Iridium(III) complexes

A wide range of iridium complexes are formed in the +3 oxidation state, the most important for iridium, with a variety of ligands. The vast majority have octahedral coordination of iridium.

The aqua ion $Ir(H_2O)_6^{3+}$ and halide complexes IrX_6^{3-} have already been mentioned above. The kinetic inertness of the low spin d^6 complexes means that hydrolysis of $IrCl_6^{3-}$ is slow: complexes up to $IrCl_2(H_2O)_4^+$ have been produced and separated from mixtures by high-voltage electrophoresis.

2.13.1 Complexes of ammines

The iridium(III) complexes are broadly similar to the rhodium(III) ammines; a selection of synthesis is shown in Figure 2.84.

As with rhodium (and cobalt), introduction of five ammonia molecules is relatively straightforward, but the sixth substitution is difficult, requiring more forcing conditions. One versatile route involves the formation of the pentammine triflate complex ion $[Ir(NH_3)_5(O_3SCF_3)]^{2+}$, where the labile triflate group is readily replaced by water, then by a range of anionic ligands [148].

A recently reported synthesis involves refluxing a mixture of $IrCl_3$ and ethanoic acid with urea; hydrolysis of the urea proceeds steadily generating the ammonia ligands. This resulting mixture of the penta-, tetra- and triammines can be separated chromatographically [149].

No structural studies have been reported on these complexes, but detailed study of their vibrational spectra permits the assignments shown in Table 2.13. Like the rhodium analogues, iridium ammines are photoactive; therefore, on excitation of ligand-field bands, solutions of $[Ir(NH_3)_6]^{3+}$ or $[Ir(NH_3)_5Cl]^+$ afford $[Ir(NH_3)_5(H_2O)]^{3+}$.

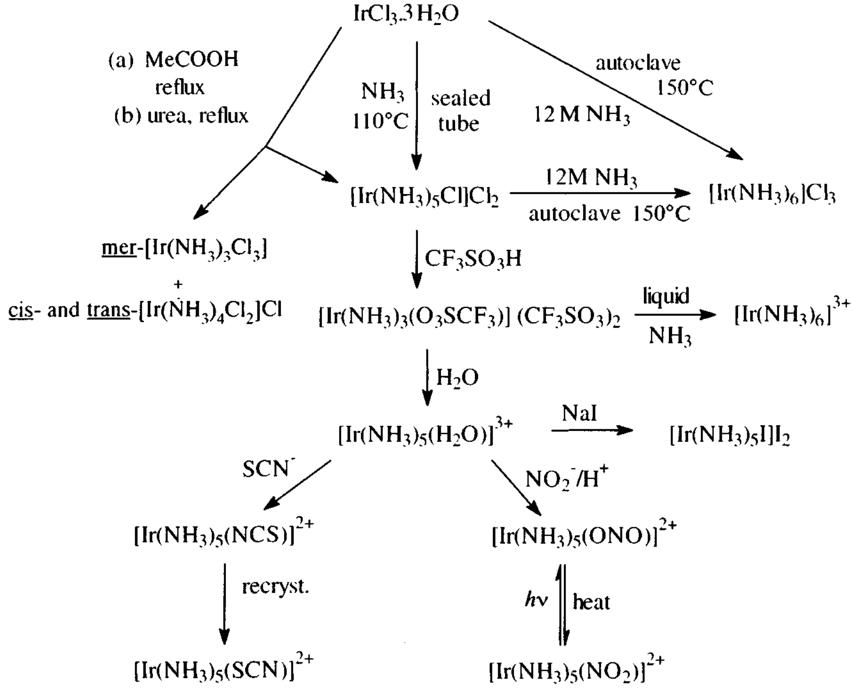

Figure 2.84 Synthesis of iridium(III) ammine complexes.

Table 2.13 Vibrational spectra of iridium(III) ammines (cm^{-1})

	ν(Ir–N)	ν(Ir–Cl)	ν(Ir–Br)
$Ir(NH_3)_6Cl_3$	527, 500, 475		
$[Ir(NH_3)_5Cl]Cl$	526, 512, 501, 479	306	
$[Ir(NH_3)_5Br]Br_2$	523, 509, 492, 478		200

Complexes with N-donor heterocyclics can be synthesized [150]:

$$IrCl_6^{3-} \xrightarrow[\text{EtOH}]{\text{py}} trans\text{-}Irpy_4Cl_2^+Cl^- \xrightarrow[\text{UV}]{\text{py}} mer\text{-}IrCl_3py_3$$

$$K_2IrCl_5(H_2O) \xrightarrow{\text{pyrazine}} K_2IrCl_5(\text{pyrazine})$$

The latter is a case of monodentate pyrazine, also found in $IrCl_3(\text{pyrazine})_3$ and $[IrCl_4(\text{pyrazine})_2]^-$.

Complexes of the bidentate ligand ethylenediamine show similar patterns to simple ammines [151]

$$Na_3IrCl_6 \xrightarrow[\text{145°C, sealed tube}]{\text{en/}H_2O} Iren_3^{3+} \xrightarrow{\text{KI}} Iren_3I_3$$

Other anions can be introduced by ion exchange. One method for bis complexes is

$$K_3IrCl_6 \xrightarrow[\text{MeCOOH}]{\text{en}} cis\text{- and } trans\text{-}Iren_2Cl_2^+Cl^-$$

The resultant mixture can be separated by fractional crystallization as the *trans*-isomer is more soluble; the *cis*-isomer can be resolved into its enantiomers using optically active anions like α-bromocamphor π-sulphonate. These chlorides can be converted into the bromide or iodide complex by refluxing with a solution of the appropriate potassium halide.

2.13.2 Complexes of S-donors

Relatively few complexes of S-donors are well characterized [152]

$$(NH_4)_2IrCl_6 \xrightarrow[\text{reflux}]{Et_2S/EtOH} fac\text{-}IrCl_3(Et_2S)_3 + [IrCl_2(Et_2S)_4]^+[IrCl_4(Et_2S)_2]^-$$

The mixture of products can be separated by dissolving the yellow neutral complex in benzene; the red 'ionic' complex is crystallized from chloroform.

Among complexes of bidentate ligands, the dithiocarbamate $Ir[S_2CN(CH_2)_4]_3$ has octahedrally coordinated iridium (Ir–S 2.38 Å) [153].

This is synthesized by a standard method, while another synthetic method uses insertion reactions:

$$K_3IrCl_6 + 3NaS_2CN(CH_2)_4 \longrightarrow Ir[S_2CN(CH_2)_4]_3 + 3KCl + 3NaCl$$

$$mer\text{-}IrH_3(PPh_3)_3 \xrightarrow{CS_2} IrH_2(S_2CH)(PPh_3)_2$$

2.13.3 Tertiary phosphine and arsine complexes

A considerable number of the tertiary phosphine and arsine complexes of iridium(III) have been synthesized [4, 8]; they generally contain 6-coordinate iridium and are conventionally prepared by refluxing Na_2IrCl_6 with the phosphine in ethanol or 2-methoxyethanol [154]

$$IrCl_6^{2-} \xrightarrow[EtOH/HCl]{PR_3} IrCl_3(QR_3)_3$$

($QR_3 = PMe_2Ph, PEt_2Ph, Et_3As, Et_2PhAs, P(alkyl)_3$, etc.). This preparation affords a mixture of the *fac*- and (principally) the *mer*-isomer of $IrCl_3(QR_3)_3$, usually with some of the salt $R_3QH^+IrCl_4(QR_3)_2^-$. Bromides and iodides can be made directly or by metathesis

$$IrBr_6^{2-} \xrightarrow[\text{butanone, heat}]{PEt_2Ph} mer\text{-}IrBr_3(PEt_2Ph)_3$$

$$mer\text{-}IrCl_3(PEt_3)_3 \xrightarrow[\text{butanone, reflux}]{NaI} mer\text{-}IrI_3(PEt_3)_3$$

The *fac*-isomers are conveniently made by a general reaction involving irradiation (fluorescent tube) of a solution of the *mer*-isomer [155]

$$mer\text{-}IrX_3(PR_3)_3 \xrightarrow[C_6H_6]{h\nu} fac\text{-}IrX_3(PR_3)_3$$

as can pseudohalide complexes

$$mer\text{-}IrCl_3(PEt_3)_3 \xrightarrow[h\nu]{Y^-/Me_2CO} fac\text{-}IrY_3(PEt_3)_3 \qquad (Y = NCS, NCO, N_3)$$

The *fac*- and *mer*-isomers can be distinguished by physical methods (IR, NMR spectra, dipole moments); they also differ in reactivity:

$$fac\text{-}IrX_3(PR_3)_3 \xrightarrow[\text{boil}]{EtOH} IrHX_2(PR_3)_3$$

The *mer*-isomer does not react under these conditions. The properties of coordinated anions (e.g. Cl^-) in these complexes depend on the *trans*-ligand in various ways. Thus in *mer*-$IrCl_3(PR_3)_3$, the chloride *trans* to phosphine is more labile and thus readily removed by aqueous $AgNO_3$ (unlike the other two chlorides). Likewise ν(Ir–Cl) in the IR spectra of these complexes depends on the ligand *trans* to chloride.

Carbon monoxide can be introduced directly

$$fac\text{-}IrCl_3(PEt_3)_3 \xrightarrow[MeO(CH_2)_2OH]{CO,\ reflux} fac\text{-}IrCl_3(CO)(PEt_3)_2$$

or by oxidative addition to iridium(I) carbonyl species

$$trans\text{-}IrBr(CO)(PEt_2Ph)_2 \xrightarrow{MeBr} IrBr_2(Me)(CO)(PEt_2Ph)_2$$

The stability of carbonyls of a metal in the +3 oxidation state is unusual; because $d\pi$–$p\pi$ back donation is necessary to stabilize the Ir–C bond, generally only one CO group can be bonded to the electron-deficient Ir^{3+}.

2.13.4 *Hydride complexes*

Hydride complexes are especially well characterized and important for iridium(III), with typical general formulae $IrHX_2L_3$, IrH_2XL_3, $IrH_3L_3$and $IrH_4L_3^+$. They are frequently readily interconvertible, as shown in Figure 2.85 for some diethylphenylphosphine complexes [156].

An 'early' preparation used 1 mol base in alcoholic solution as the reducing agent:

$$mer\text{-}IrCl_3(PEt_3)_3 + KOH + C_2H_5OH$$
$$\xrightarrow{boil} IrHCl_2(PEt_3)_3 + KCl + H_2O + MeCHO$$

(The ethanal was converted to its 2,4-DNP derivative, obtained in 87% yield.) It may also be noted that for this redox reaction, iridium retains the +3 state throughout. The more labile chloride *trans* to phosphine is replaced

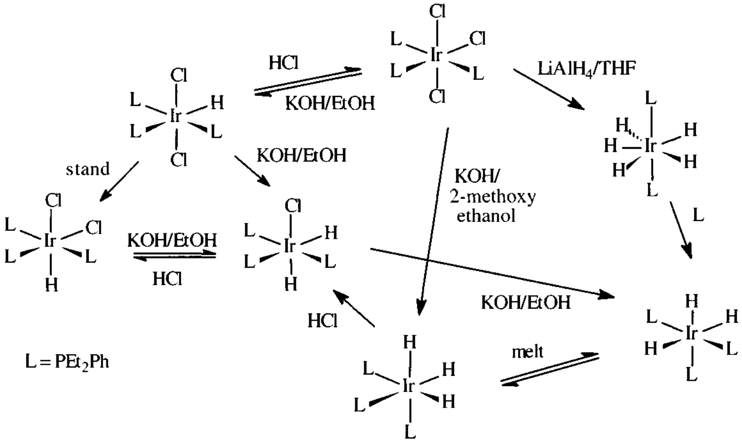

Figure 2.85 Iridium hydrido complexes.

in the reaction; reaction of HCl with the hydride regenerates the starting complex.

Extended reflux with larger quantities of base, especially in higher-boiling alcohols, can afford di- and trihydrides, while oxidative addition can be used

$$Ir(PMe_2Ph)_4^+ + H_2 \rightarrow IrH_2(PMe_2Ph)_4^+$$

With bulky phosphines, 6-coordinate structures are not possible [157]

$$IrCl_6^{3-} \xrightarrow[\text{reflux}]{\text{exc. PBu}^t_2\text{R}} IrHCl_2(PBu^t_2R)_2$$

$$IrCl_3.3H_2O \xrightarrow[\text{EtOH reflux}]{\text{HCl/PPr}^i_3} IrHCl_2(PPr^i_3)_2$$

These compounds are generally believed to have square pyramidal structures (X-ray, PPr^i_3) [157d] and have typical spectroscopic properties of transition-metal hydrides ($IrHCl_2(PBu^t_2Me)_2$ $\nu(Ir{-}H)$ 1998 cm^{-1}).

$Ir(H)_2X(PBu^t_2R)_2$ (X = Cl, Br, I; R = Me, Ph) has a tbp structure (axial phosphines) (Ir–H 1.512–1.553 Å for X = Cl, R = Ph) but is fluxional in solution [157e]. Low-temperature NMR studies indicate hindered rotation about Ir–P bonds in $IrHCl_2(PBu^t_2Me)_2$ [158]. $IrH_2Cl(PPr^i_3)_2$ undergoes HID exchange with deuterated solvents and acts as an alkane dehydrogenation catalyst [159].

Trihydrides can be made more readily by using $LiAlH_4$ or $NaBH_4$ as reducing agents:

$$IrCl_3(QR_3)_3 \xrightarrow[\text{THF}]{\text{NaBH}_4\text{ or LiAlH}_4} IrH_3(QR_3)_3$$

(PR_3, e.g. PPh_3, PEt_2Ph, PMe_2Ph, $AsEt_2Ph$). These preparations afford mixtures of the *fac*- and *mer*-isomers, separable by fractional crystallization and distinguishable spectroscopically. Figure 2.86 show the ^1H NMR spectrum in the hydride region of the two isomers of $IrH_3(PEt_2Ph)_3$ [160].

Trihydrides lose some or all of the hydride ligands with suitable reagents

$$IrH_3(PPh_3)_3 \xrightarrow{\text{HBr}} IrHBr_2(PPh_3)_3$$

The structures of *fac*-$IrH_3(PMe_2Ph)_3$, $IrH_2Cl(PMe_2Ph)_3$ and $IrHCl_2(PMe_2Ph)_3$ (2-isomers) have been determined (see section 2.13.5) as well as those of *mer*-$IrH_3(PPh_3)_3$ and *fac*-$IrH_3(PMePh_2)_3$ (Figure 2.87) [161]. They all involve octahedrally coordinated iridium, with hydride ligands occupying individual positions in the coordination sphere.

Protonation of *mer*-$IrH_3(PMe_2Ph)_3$ with HBF_4 leads to $[IrH_4(PMe_2Ph)_3]^+$, believed to be a non-classical hydride $[IrH_2(\eta^2\text{-}H_2)(PMe_2Ph)_3]^+$ [162]. It catalyses *fac–mer* isomerism of $IrH_3(PMe_2Ph)_3$. $IrHCl_2L_2$ (L = Pcy_3, PPr^i_3)

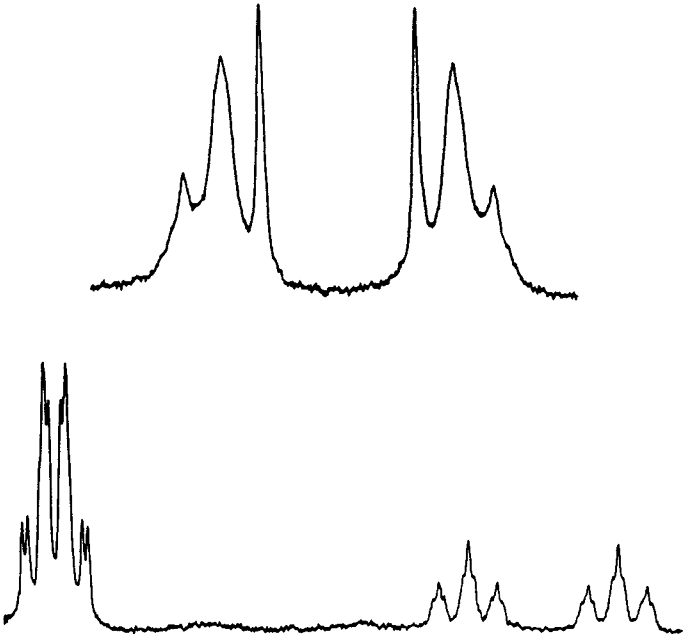

Figure 2.86 The ^1H NMR spectrum in the hydride region of the isomers of $[IrH_3(PEt_2Ph)_3]$: top, *fac*-isomer; bottom, *mer*-isomer. (Reproduced with permission from E.L. Muetterties (ed.), *Transition Metal Hydrides*, published by Marcel Dekker, 1971, p. 80.)

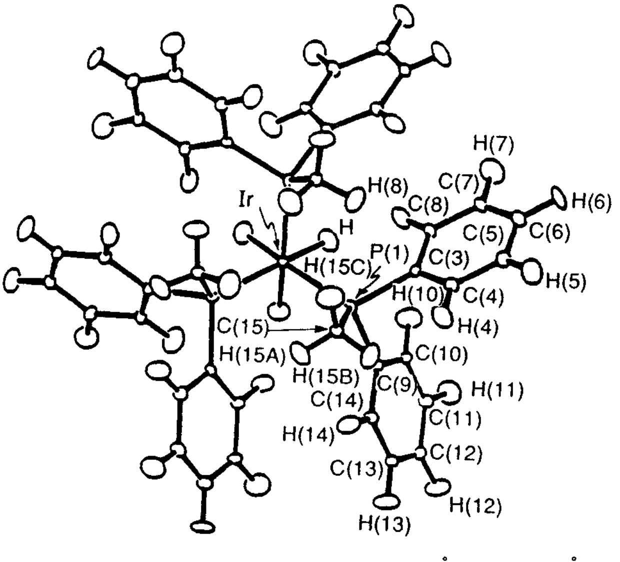

Figure 2.87 The structure of *fac*-$[IrH_3(PPh_2Me)_3]$. Ir–H 1.627 Å, Ir–P 2.314 Å; H–Ir–H 83.4°, P–Ir–P 98.6°. (Reproduced with permission from *J. Chem. Soc., Dalton Trans.*, 1993, 3359.)

reversibly binds H_2, probably as another η^2-hydrogen complex $IrH(\eta^2\text{-}H_2)Cl_2(PR_3)_2$.

Formally iridium(V) hydrides are discussed in section 2.15.

2.13.5 Case study of dimethylphenylphosphine complexes

The PMe_2Ph complexes have been studied in particular detail [163–165], since their ^1H NMR spectra lend themselves to assigning the stereochemistry of the complexes. Figure 2.88 shows the relationships between a large number of these complexes, which are in general typical of iridium(III) phosphine complexes.

The initial synthesis of $IrCl_3(PMe_2Ph)_3$ leads mainly to the *mer*-isomer (I) (and a certain amount of the $(HPMe_2Ph)^+[IrCl_4(PMe_2Ph)_2]^-$ (III) byproduct), which can be isomerized to the *fac*-isomer (II) by irradiation (section 2.13.3) [104]. Refluxing in alcohols, particularly in the presence of base, leads to hydride complexes (V and VI): the labilizing effect of the phosphine on the chloride *trans* to it should be noted in the synthesis of (V). Hydride ligands can be replaced by halide or pseudo-halide (VIII); a hydride (VII) isomeric with (V) can be produced by treatment of (VI) with HCl; in this case only the hydride *trans* to phosphine is replaced. In contrast, *fac*-$IrCl_3(PMe_2Ph)_3$ (II) requires gentle boiling in ethanol for a few hours to introduce a hydride ligand giving (XIII).

An indication of the *trans*-labilizing influence of phosphine is given by the reaction of *mer*-$IrCl_3(PMe_2Ph)_3$ with NaI; the chloride *trans* to phosphines is replaced within 3.5 h reflux in butanone, forming VIII ($X = I$) whereas 48 h reflux is needed to replace all three chlorides (forming XIV).

Another way of replacing chloride *trans* to phosphine involves using silver salts; reaction with $AgPF_6$ and $AgNO_3$ introduces, respectively, a water molecule (XII) and a nitrate group (IX), which may in turn be replaced by a range of Lewis bases, giving (VIII), (X) and (XXV).

The cationic species $[IrX_2(CO)(PMe_2Ph)_3]^+$ (XVI, $Q = CO$) undergoes nucleophilic attack by methoxide forming the carboxylate complex (XXI). In the presence of very strong base, a cyclometallation of a methyl group occurs forming (XXIV) [165].

One or more methyl groups can be introduced. Using excess MeMgCl results in a change in configuration from *mer*- to *fac*-(XVIII); replacing one or two of these methyl groups results in the readoption of the *mer*-configuration for the phosphines (XIX, XX). (Presumably the *mer*-configuration is more stable for $d\pi$–$p\pi$ bonding but this has to be balanced against electronic and other steric factors [166].)

Variable temperature NMR studies of $[IrCl_2(PMe_2Ph)_4]^+$ (XXV; $L = PMe_2Ph$) show a broad line in the ^{31}P spectrum at room temperature but on cooling to 80°C a mass of sharp lines are observed, owing to three to four rotational isomers (Figure 2.89); the predominant ABCD pattern is

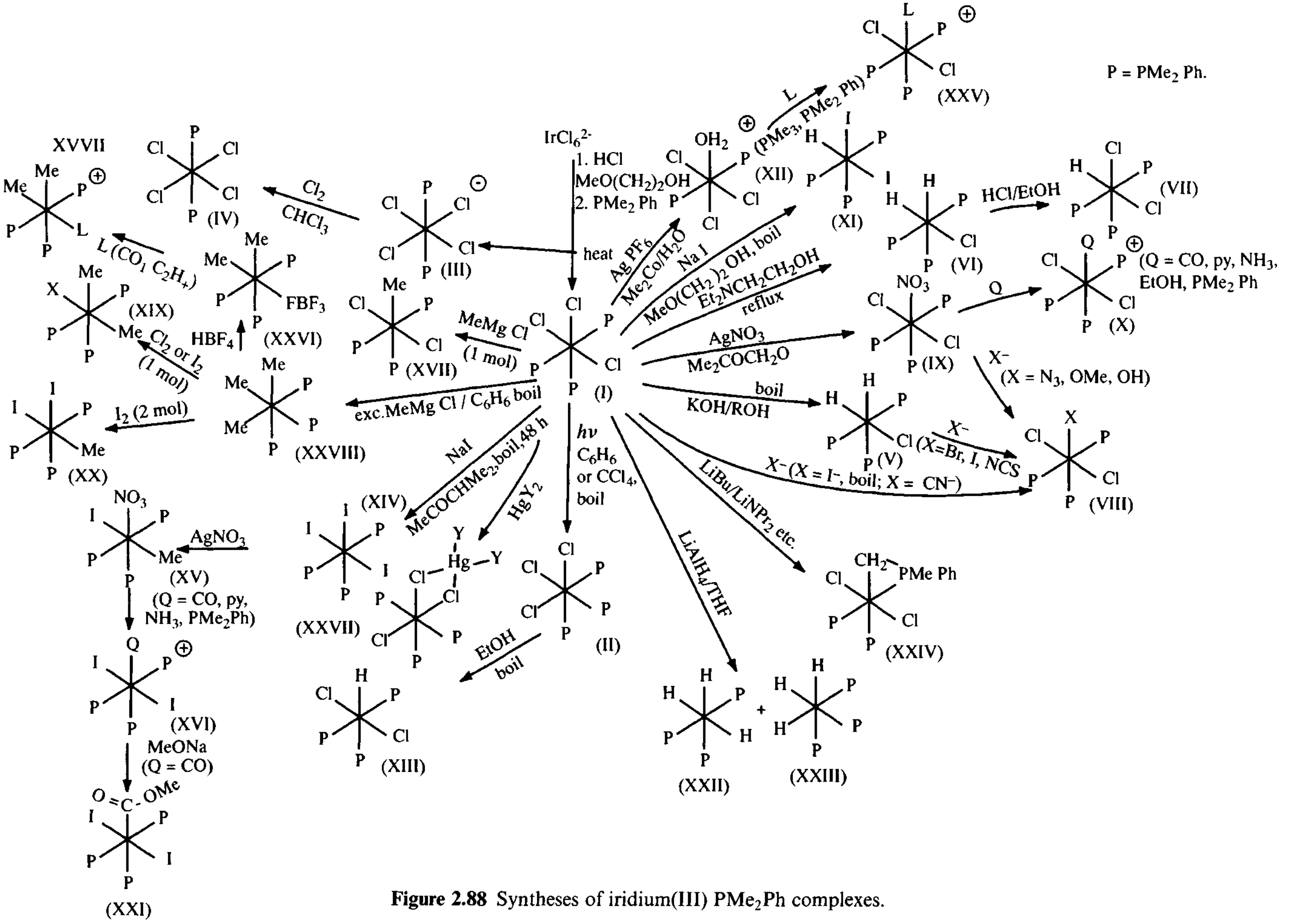

Figure 2.88 Syntheses of iridium(III) PMe$_2$Ph complexes.

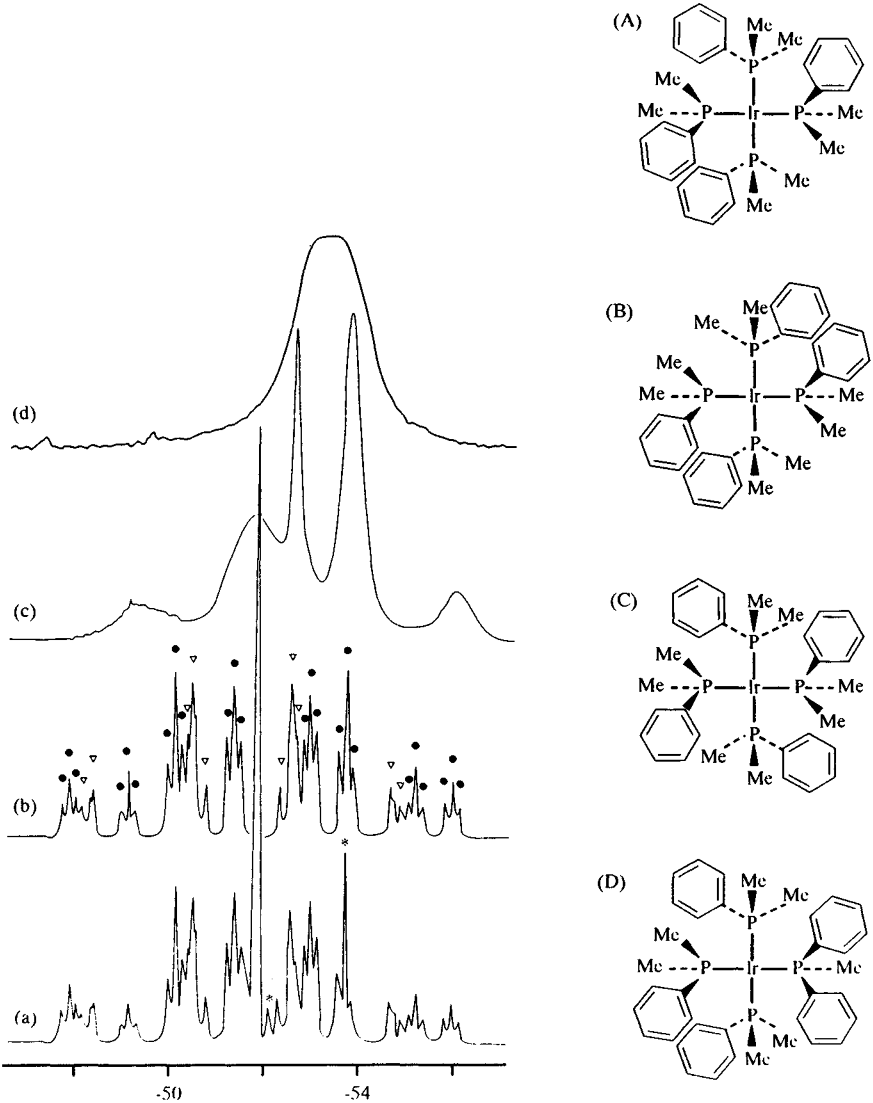

Figure 2.89 $^{31}P\{^1H\}$ NMR spectrum of $[IrCl_2(PMe_2Ph)_4]^+ClO_4$ at (a) −80°C; (c) −5°C; and (d) 25°C; together with a computer simulation (b). Signals owing to rotameric isomers are denoted •, ▽ and *. The four possible rotamers are shown as A–D. (Reproduced with permission from *J. Chem. Soc., Chem Commun.*, 1989, 1351.)

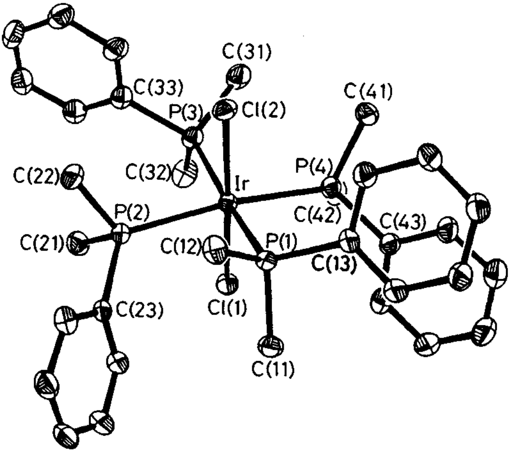

Figure 2.90 The structure of the cation in $[IrCl_2(PMe_2Ph)_4]ClO_4$. (Reproduced with permission from *J. Chem. Soc., Chem Commun.*, 1989, 1351.)

assigned to isomer A, the form adopted in the solid state (Figure 2.90). (One interesting point about this substance is the phenomenon of parallel phenyl groups (3.8 Å apart) noted in certain other substances like *cis*-$UCl_4(Ph_3PO)_2$ [167].)

As already remarked, in compounds *mer*-$IrX_3(PMe_2Ph)_3$, the most labile ligand is the group X (X = H, Me, halogen) *trans* to a phosphine. The Ag^+-assisted removal of chloride in (I) yields $[IrCl_2(H_2O)(PMe_2Ph)_3]^+$ (XII) where the H_2O is very weakly bound (Ir–O 2.189 Å, compare $Ir(H_2O)_6^{3+}$ 2.041 Å) and readily replaced.

Similarly protonation of *fac*-$IrMe_3(PMe_2Ph)_3$ with HBF_4 gives $IrMe_2(BF_4)(PMe_2Ph)_3$ (XXVI), which has weakly bound BF_4 (Ir–F 2.389 Å): in solution the BF_4 is easily displaced by neutral donors to give (XXVII) [168].

Structural data

Figure 2.91 compares bond lengths for a range of these complexes [169]. Comparison of Ir–P bond lengths (e.g. for compounds I, II and V) shows the shortest Ir–P bonds *trans* to Cl and the longest for P *trans* to H. A similar effect is seen on Ir–Cl bond lengths by comparing the same compounds.

Examining the *mer*-$IrH_{3-x}Cl_x(PMe_2Ph)_3$ systems (I, V, VI, VII) it has been noted that the Ir–P bonds *trans* to a particular ligand shorten as the number of hydride ligands increases (increments of about 0.04 Å). This is not simply caused by interligand repulsions as the Ir–Cl bonds do not show this variation; it has been concluded that both non-bonding interligand forces and metal–ligand bonding forces are involved. Comparing

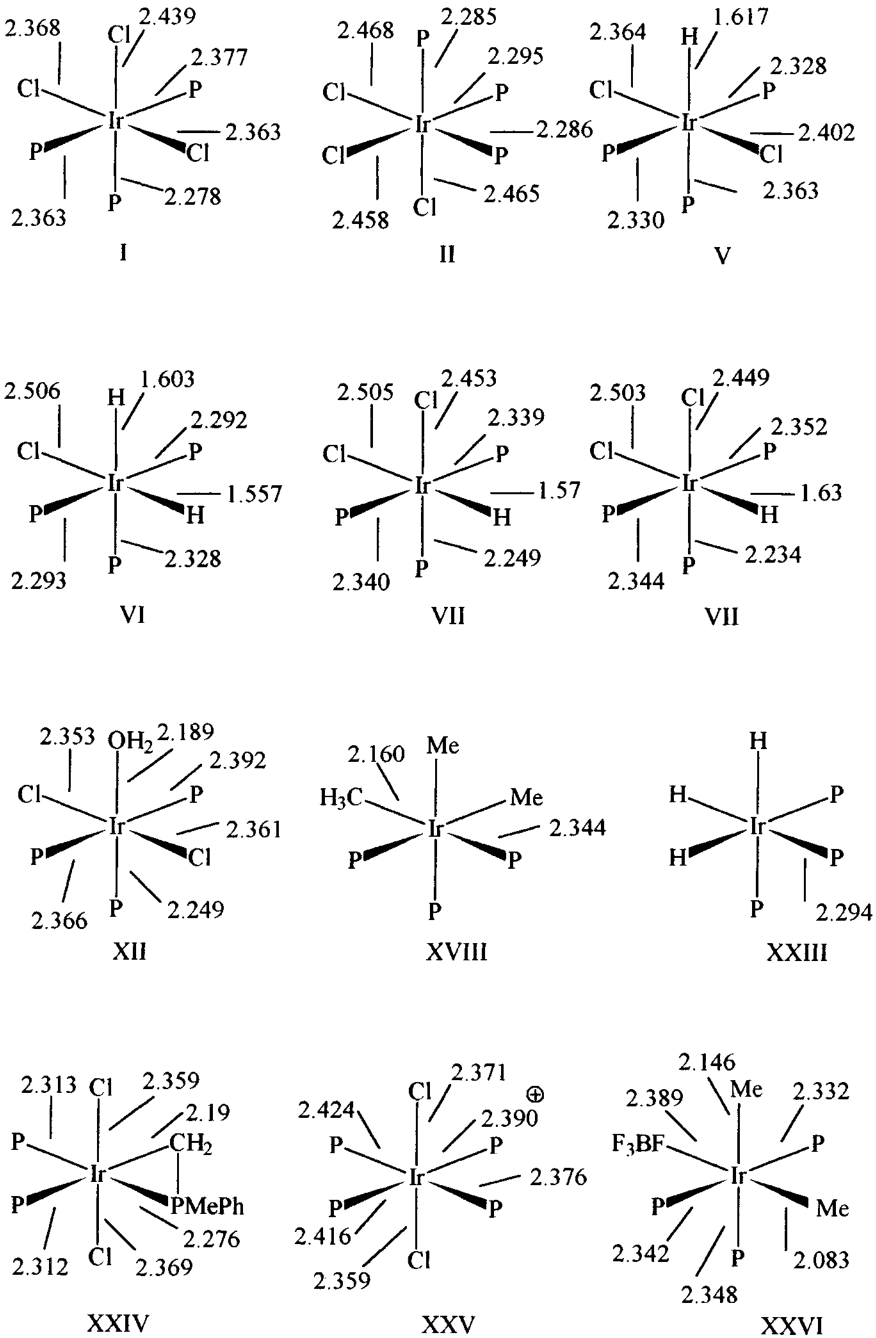

Figure 2.91 Structural data for iridium(III) complexes of dimethylphenylphosphine.

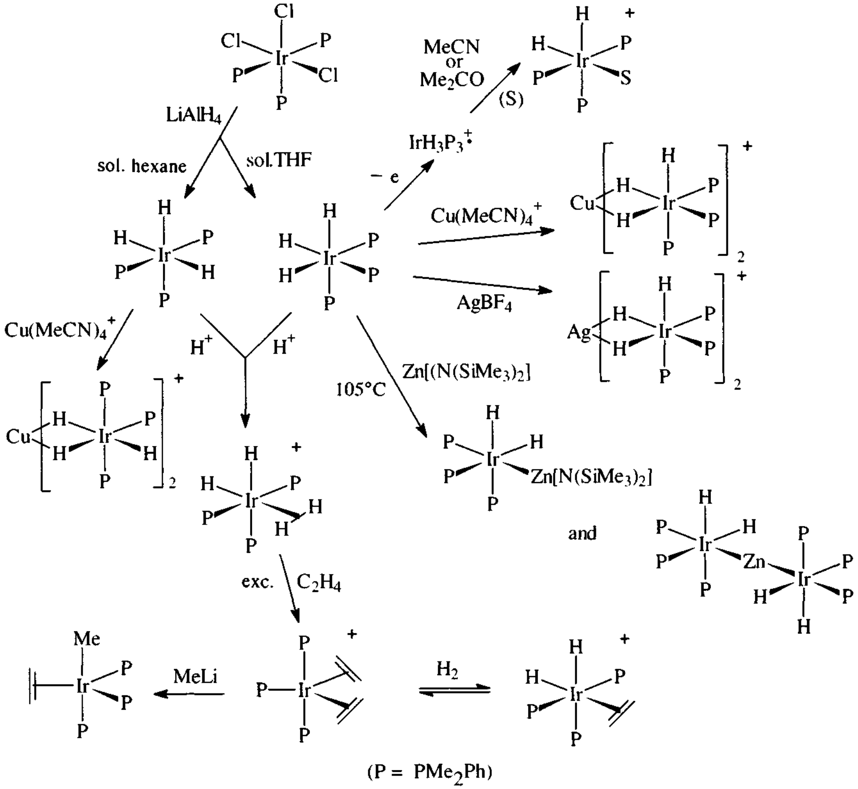

Figure 2.92 Reactions of iridium(III) dimethylphenylphosphine trihydro and trimethyl complexes.

fac-$IrX_3(PMe_2Ph)_3$ compounds (X = Cl, H, Me: II, XXIII and XVIII) shows a very significant effect of methyl on the Ir–P bond.

Recent study of these complexes has focused on the reactions of trimethyls and trihydrides (Figure 2.92) as on protonation they generate reactive co-ordinatively unsaturated species

$$IrX_3P_3 \xrightarrow{H^+} IrHX_3P_3^+ \rightarrow IrXP_3^+ + HX \qquad (X = H, Me)$$

$LiAlH_4$ reduction of *mer*-$IrCl_3(PMe_2Ph)_3$ gives a separable mixture of *fac*- and *mer*-$IrH_3(PMe_2Ph)_3$ (XXII and XXIII); these are rigid 6-coordinate complexes (readily binding electrophilic complexes like $Cu(MeCN)_4^+$ to form hydride-rich clusters) but on protonation (HBF_4) they form $[IrH_4(PMe_2Ph)_3]^+$, which appears to be the dihydrogen complex $[Ir(\eta^2\text{-}H_2)H_2(PMe_2Ph)_3]^+$: similar intermediates $[IrMe_2(PMe_2Ph)_3]^+$ can be made by protonation of $IrMe_3(PMe_2Ph)_3$ [170].

2.14 Iridium(IV) complexes

The chemistry of the iridium +4 oxidation state is limited, owing to the stability of the low-spin d^6 Ir^{3+} complexes, which makes their oxidation difficult. The best known are IrX_6^{2-} ($X = F, Cl, Br$) (see section 2.3).

A variety of complexes of neutral donors IrX_4L_2 have been made [171]:

$$IrX_3.nH_2O \xrightarrow[HX/EtOH]{L} HL + IrX_4L_2^- \xrightarrow[CHCl_3]{X_2} IrX_4L_2$$

($X = Cl$, $L = PMe_3, PMe_2Ph, PEt_3, PEt_2Ph, PPr_3, AsPr_3$, py)
($X = Br$, $L = PEt_3, AsEt_3, PMe_2Ph, AsMe_2Ph$, py)

$$IrX_3.nH_2O \xrightarrow[HX, L]{R_4NX} R_4N^+IrX_4L_2^- \xrightarrow{X_2} IrX_4L_2$$

($X = Cl$, $L = Me_2S, Me_2Se$; $X = Br$, $L = Me_2S$)

$$[Ir(C_8H_{12})Cl]_2 \xrightarrow{PPh_3} Ir(PPh_3)_3Cl \xrightarrow{Cl_2} IrCl_4(PPh_3)_2$$

The choice of starting material is important, as IrX_3L_3 (L, e.g. PR_3) usually cannot be oxidized.

The complexes are strongly coloured (purple chlorides, green bromides) light-sensitive solids that undergo facile reduction. In general, only the *trans*-isomer is formed (though *cis*-$IrCl_4py_2$ has been made by oxidizing the corresponding iridium(III) species). Magnetic and spectroscopic properties are as expected for a low-spin d^5 system, magnetic moments at room temperature being in the range 1.6–1.9 μ_B; *trans*-$IrCl_4(AsPr_3)_2$ shows the ESR spectrum expected for a *trans*-isomer ($g_\perp = 2.43$, $g_\| = 0.80$).

Comparison of the far-IR spectra of the two isomers of $IrCl_4py_2$ shows two ν(Ir–Cl) bands for the *trans*-isomer (330, 317 cm^{-1}) and three for the *cis*-isomer (346, 328, 272 cm^{-1}), as predicted by group theory. The *trans*-geometries are confirmed by X-ray diffraction for $IrCl_4(PMe_2Ph)_2$ (Ir–Cl 2.324 Å, Ir–P 2.392 Å) and $IrBr_4(AsEt_3)_2$ (Ir–Br 2.459 Å, Ir–As 2.489 Å) (Figure 2.93).

The *cis*-complexes can be made using chelating bidentate ligands, the syntheses again following the route of oxidation of the iridium(III) analogue.

$$IrX_3.nH_2O \xrightarrow[L-L]{HX} Ir(L-L)X_4^- \xrightarrow[\text{or } HNO_3]{X_2} IrX_4(L-L)$$

(L–L = phen, bipy, $X = Cl, Br$)

$$IrCl_3.nH_2O \xrightarrow{L-L} Ir(L-L)Cl_3 \xrightarrow{R_4NCl} Ir(L-L)Cl_4^- \xrightarrow{X_2} Ir(L-L)Cl_4$$

(L–L = $RQ(CH_2)_2QR$ ($R = Me, Ph$; $Q = S, Se$); $MeS(CH_2)_3SMe$).

The structure of *cis*-$Ir(phen)Cl_4$ is shown in Figure 2.94.

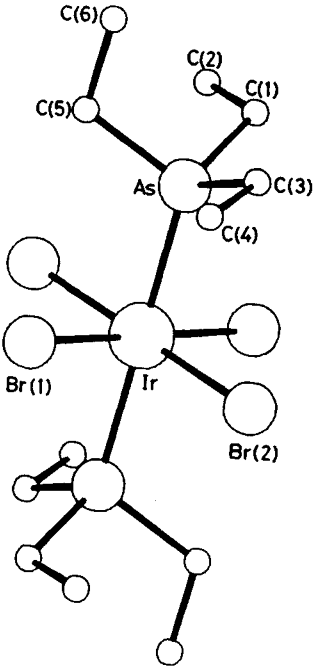

Figure 2.93 The structure of *trans*-[$Ir(AsEt_3)_2Br_4$]. (Reproduced with permission from *J. Chem. Soc., Dalton Trans.*, 1987, 1901.)

Anionic complexes $Et_4N[IrCl_5L]$ (L = py, Me_2S, Me_2Se, PPh_3, $AsPh_3$, $SbPh_3$) have been synthesized:

$$trans\text{-}IrCl_4py_2 \xrightarrow[CH_2Cl_2]{HCl/Et_4NCl} Et_4NIrCl_5py$$

$$\xrightarrow[3.\ Cl_2/CH_2Cl_2]{1.\ reduce;\quad 2.\ L,\ EtOH} Et_4NIrCl_5L$$

These iridium(IV) complexes have UV–visible spectra dominated by intense absorptions around 500 nm (X = Cl) and 700 nm (X = Br) assignable to $\pi x \rightarrow Ir(t_{2g})$ ligand-to-metal charge-transfer bonds.

$IrCl_4(PMe_2Ph)_2$ undergoes a redox reaction with ferrocene forming

$[Fe(C_5H_5)_2]^+[IrCl_4(PMe_2Ph)_2]^-$

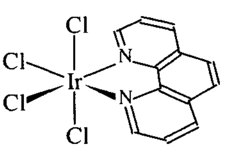

Figure 2.94 The structure of *cis*-$Ir(phen)Cl_4$.

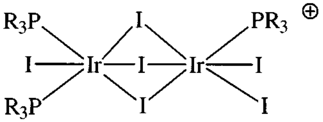

Figure 2.95 The structure of the dimeric cation $[Ir_2I_5(PR_3)_4]^+$.

No IrI_4 complexes have so far been characterized: $Ir(PR_3)_4^+$ ($PR_3 = PMe_2Ph$, $P(OMe)Ph_2$) is oxidized by iodine giving complexes analysing as $IrI_4(PR_3)_2$. They are in fact dimeric iridium(III) complexes $Ir_2I_5(PR_3)_4^+I_3^-$, containing the cation shown in Figure 2.95 [122a].

Recently two rare paramagnetic iridium(IV) hydride complexes have been reported [172].

$$(NH_4)_2IrCl_6 \xrightarrow[\text{EtOH/conc. HCl}]{PR_3} IrH_2Cl_2(PR_3)_2 \qquad (R = Pr^i, cy)$$

As expected, they are deeply coloured ($R = Pr^i$, deep red; $R = cy$, red–violet) and have typical magnetic moments of 1.5–$1.6\,\mu_B$ and ESR g values 2.064, 2.038, 2.007 (for $R = Pr^i$); others [157d] have suggested that the structures were obtained on disordered molecules. In solution, at room temperature, they tend to decompose

$$2IrH_2Cl_2(PR_3)_2 \Leftrightarrow IrHCl_2(PR_3)_2 + IrH(\eta^2\text{-}H_2)Cl_2(PR_3)_2$$

$Ir(OH)_6^{2-}$ is formed by a substitution reaction and is isolable as red crystals. Similar complexes have been isolated for the heavier group (II) metals.

$$K_2IrCl_6 \xrightarrow{KOH} K_2Ir(OH)_6$$

On heating they afford M_2IrO_3 ($M = Na$, K; $\frac{1}{2}Ca$, $\frac{1}{2}Sr$, $\frac{1}{2}Ba$), which can in some cases be made by heating the appropriate metal oxide with IrO_2, though M_2IrO_4 ($M = Ca$, Sr) can also be made. All probably have 6-coordinate Ir^{4+} [173].

Red moisture-sensitive crystals of $K_2Ir(NO_3)_6$, isomorphous with the Pt analogue and believed to contain 12-coordinate iridium, with bidentate nitrates are made by:

$$K_2IrBr_6 \xrightarrow{N_2O_5} K_2Ir(NO_3)_6$$

The rubidium and caesium analogues can also be synthesized [174].

The mixed valence (III, IV) ions $Ir_3N(SO_4)_6(H_2O)_3^{4-}$ and $Ir_3O(SO_4)_9^{10-}$ have been made by reactions of H_2SO_4 with $(NH_4)_2IrCl_6$ and K_2IrCl_6, respectively. They have structures similar to trinuclear carboxylates $M_3O(RCO_2)_6(H_2O)_3^{n+}$ based on Ir_3X cores with bridging sulphates.

2.15 Iridium(V) complexes

Compounds $IrH_5(PR_3)_2$ (PR_3, e.g. PEt_2Ph, PMe_3, PEt_3, PPr^i_3) are prepared by $LiAlH_4$ reduction of THF solutions of $IrCl_3(PR_3)_3$ or $IrHCl_2(PPr^i_3)_2$. ($IrH_5(PEt_2Ph)_2$ was originally though to be a trihydride on the basis of analytical data.)

$$IrCl_3(PR_3)_3 \xrightarrow[\text{THF}]{LiAlH_4 \text{ or } NaBH_4} IrH_5(PR_3)_2$$

Other syntheses include

$$IrHCl_2(PBu^t_2R) \xrightarrow[C_6H_6]{NaOPr^i/H_2} IrH_5(PBu^t_2R)_2 \qquad (R = Me, Ph, Bu^t)$$

Two hydrogen atoms are readily displaced by a molecule of a Lewis base

$$IrH_5(PEt_3)_2 + AsMe_2Ph \rightarrow mer\text{-}IrH_3(PEt_3)_2(AsMe_2Ph) + H_2$$

$$IrH_5(PEt_2Ph)_2 + L \rightarrow mer\text{-}IrH_3(PEt_2Ph)_2L + H_2$$

($L = PPh_3$, $AsMe_2Ph$, MeNC, Me_2S, CO).

The facile displacement of H_2 might suggest that the pentahydrides were dihydrogen complexes of iridium(III), $IrH_3(\eta^2\text{-}H_2)(PR_3)_2$. However, the structure of $IrH_5(PPr^i_3)_2$ has been determined by X-ray and neutron diffraction (Figure 2.96), showing the molecule to be pentagonal bipyramidal with *trans*-phosphines and five equivalent equatorial hydrides (Ir–P 2.309 Å; Ir–H 1.603 ± 0.025 Å) [175].

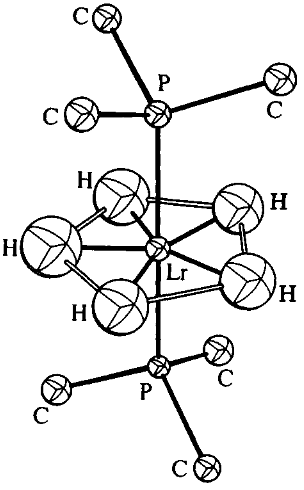

Figure 2.96 The structure of $IrH_5(PPr^i_3)_2$. (Reprinted with permission from *J. Am. Chem. Soc.*, 1985, **107**, 7212. Copyright (1985) American Chemical Society.)

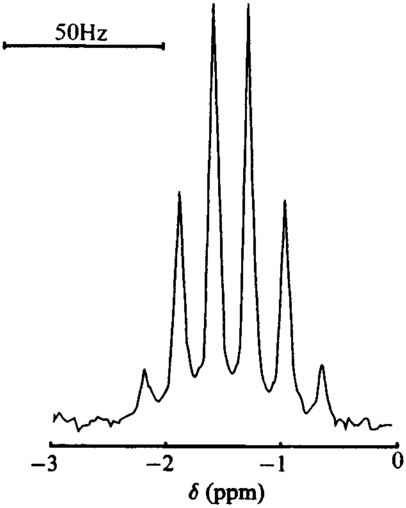

Figure 2.97 ^{31}P NMR spectrum (ethyl protons decoupled) of $IrH_5(PEt_2Ph)_2$. (Reprinted from *J. Inorg. Nucl. Chem.*, 1973, **33**, 2195. Copyright (1973) with kind permission from Elsevier Science Ltd, The Boulevard, Langford Lane, Kidlington OX5 1GB, UK.)

The IR spectrum shows ν(Ir–H) at 1950 cm^{-1} and a triplet in the ^1H NMR at $\delta = -11$ ppm (J(P–H) 12 Hz) confirming the presence of two phosphines. The ^{31}P NMR of $IrH_5(PEt_2Ph)_2$ (Figure 2.97) is a sextet, showing the presence of five hydride ligands.

These pentahydrides have attracted attention as catalysts for hydrogenation of the double bond in alkenes. $IrH_5(PPr^i_3)_2$ catalyses vinylic H–D exchange between terminal alkenes and benzene, the isomerization of α,β-ynones, isomerization of unsaturated alcohols and dehydrogenation of molecules such as secondary alcohols [176].

Recently an orange compound $IrH_4Cl(PPr^i_3)_2$ has been isolated (IR ν(Ir–H) 2204 and 2152 cm^{-1}) as has the Pcy_3 analogue [177].

$$IrCl_3.3H_2O \xrightarrow[\text{Na naphthalenide}]{H_2/PPr^i_3/THF} IrH_4Cl(PPr^i_3)_2$$

It is stable in the solid state only under a hydrogen atmosphere, tending to eliminate H_2 reversibly.

$$IrH_4Cl(PPr^i_3)_2 \underset{+H_2}{\overset{-H_2}{\rightleftharpoons}} IrH_2Cl(PPr^i_3)_2 + H_2$$

X-ray diffraction has not located the hydrides, but NMR evidence favours a structure of the type (Figure 2.98) with one (η^2-H_2) ligand.

Protonation of $IrH_5(Pcy_3)_2$ affords a fluxional complex thought to be $IrH_6(Pcy_3)_2^+$ with two (η^2-H_2) ligands and two classical hydrides (Figure 2.99) from the ^1H NMR ($\delta = -8.3$ ppm at room temperature;

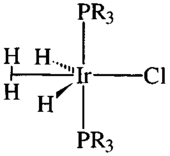

Figure 2.98 The structure of $IrH_4Cl(PR_3)_2$.

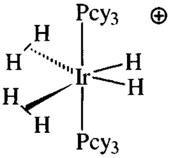

Figure 2.99 The structure of $[IrH_6(Pcy_3)_2]^+$.

$\delta = -5.05$ ppm (intensity 4) and -15.2 ppm (intensity 2) at low temperature). It can, therefore, be viewed as an iridium(III) complex [178].

2.16 Nitrosyls of iridium and rhodium

Two factors have contributed particularly to the interest in the iridium and rhodium nitrosyl compounds [179]:

1. The report in 1968 of the first crystallographically characterized bent metal–nitrosyl linkage in $[IrCl(NO)(CO)(PPh_3)_2]^+BF_4^-$ [180].
2. The discovery that $[Ir(NO)_2(PPh_3)_2]^+$ reacts with CO forming the carbonyl $Ir(CO)_3(PPh_3)_2^+$, which then regenerates the starting material in reacting with NO [181]

$$Ir(NO)_2(PPh_3)_2^+ + 4CO \rightarrow Ir(CO)_3(PPh_3)_2^+ + CO_2 + N_2O$$

$$Ir(CO)_3(PPh_3)_2^+ + NO \rightarrow Ir(NO)_2(PPh_3)_2^+$$

This has obvious potential for removing undesirable NO and CO from automobile exhaust gases.

Bent metal–NO bonding is traditionally associated with NO bonding as NO^-, whereas linear coordination is associated with NO^+. The latter is predicted to involve shorter M–N bonds as both σ- and π-donation can be involved.

$$Ir{-}N^+{\equiv}O^-: \qquad Ir{=}N^+{=}\ddot{O}:$$

On this basis, the bent nitrogens with square pyramidal structures like $Ir(NO)Cl_2(PPh_3)_2$ are assigned to the M^{III} (d^6) oxidation state in keeping with other examples of this stereochemistry, such as $RhCH_3I_2(PPh_3)_2$.

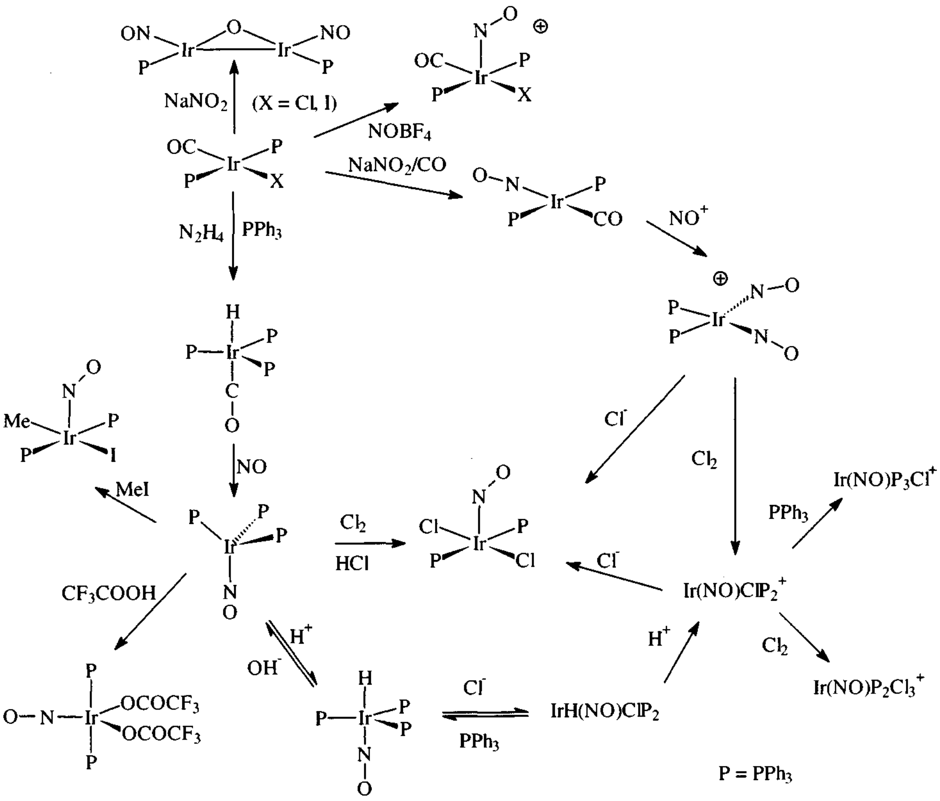

Figure 2.100 Synthesis of some iridium nitrosyl complexes.

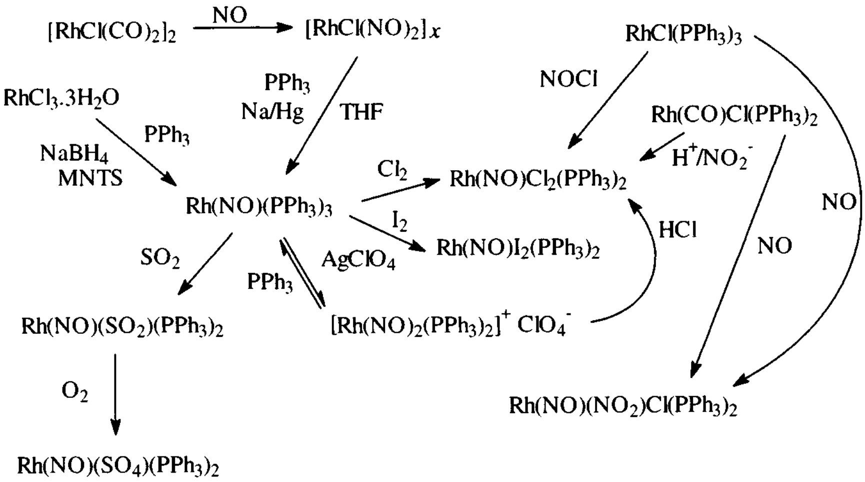

Figure 2.101 Synthesis of some rhodium nitrosyl complexes.

Table 2.14 Structural data for iridium nitrosyl complexes

	Ir–N (Å)	Ir–N–O (°)	ν(NO) (cm^{-1})
$Ir(NO)(PPh_3)_3$	1.67	180	1600
$[IrH(NO)(PPh_3)_3]^+ClO_4^-$ (black isomer)	1.68	175	1780
(brown isomer)	1.77	167	1720
$[IrCl(NO)(PPh_3)]_2O$	1.77	176	1831–1854
$[Ir(NO)_2(PPh_3)_2]^+ClO_4$	1.77	164	1715–1760
$[Ir(NO)(\eta^3\text{-}C_3H_5)(PPh_3)_2]^+BF_4^-$	1.95	129	1631
$[IrI(NO)(CO)(PPh_3)_2]^+BF_4^-$	1.89	125	1720
$[IrCl(NO)(CO)(PPh_3)_2]^+BF_4^-$	1.97	124	1680
$IrCl_2(NO)(PPh_3)_2$	1.94	123	1560
$IrI(NO)CH_3(PPh_3)_2$	1.92	120	1525
$[Ir(NO)(phen)(PPh_3)_2]^{2+}(PF_6)_2$	1.70	180	1805
$Ir(NO)(O_2CCF_3)_2(PPh_3)_2$	1.59	178	1800
$Ir(NO)(CO)(PPh_3)_2$	1.787	174	1645
$K_2Ir(NO)Cl_5.H_2O$	1.760	174	2006

It has frequently been assumed that linear M–N–O linkages are associated with higher ν(N–O) frequencies than bent M–NO linkages. Unfortunately there is a region of overlap between (roughly) 1600 and 1720 cm^{-1} where both linkages have been found to absorb. X-ray diffraction and, latterly, ^{15}N NMR spectra have been most useful in resolving the situation [182].

Syntheses of many of these compounds are shown in Figures 2.100 and 2.101, with structural data in Tables 2.14 and 2.15. Apart from NO itself, convenient reagents for introducing the group include NO^+ salts and MNTS (*N*-methyl-*N*-nitrosotoluene-*p*-sulphonamide, *p*-$MeC_6H_4SO_2N(NO)Me$).

$[IrCl(NO)(PPh_3)_2]^+$ is the nitrosyl analogue of Vaska's compound [183]. These are various synthetic routes to it

$$[IrH(NO)Cl(PPh_3)_2]^+ \xrightarrow{HX} [IrCl(NO)(PPh_3)_2]^+X^- + H_2$$

Table 2.15 Structural data for rhodium nitrosyl complexes

	Rh–N (Å)	Rh–N–O (°)	ν(NO) (cm^{-1})
$[Rh(NO)_2(PPh_3)_2]^+ClO_4^-$	1.818	159	1754, 1759
$Rh(NO)(PPh_3)_3$	1.759	157	1610
$Rh(NO)(\eta^2\text{-}SO_2)(PPh_3)_2$	1.802	140.4	1600
$Rh(NO)Cl_2(PPh_3)_2$	1.912	124.8	1630
$Rh(NO)(O_2CCF_3)_2(PPh_3)_2$	1.93	122	1665
$[Rh(NO)(MeCN)_3(PPh_3)_2]^{2+}[PF_6^-]_2$	2.026	118	1720

($X = ClO_4$, PF_6, BF_4) (note the hydrogen bound to iridium behaving here as H^-).

$$IrCl(CO)(PPh_3)_2 \xrightarrow{RCON_3} IrCl(N_2)(PPh_3)_2 \xrightarrow{NO^+BF_4^-} [IrCl(NO)(PPh_3)_2]^+$$

This synthesis is possible with other halide ligands

$$[Ir(NO)_2(PPh_3)_2]^+ \xrightarrow[(1\,mol)]{Cl_2} [IrCl(NO)(PPh_3)_2]^+$$

Counting NO as a three-electron donor, $[IrCl(NO)(PPh_3)_2]^+$ is, therefore, a 16-electron species isoelectronic with Vaska's compound, isolable as a red crystalline hexafluorophosphate (m.p. 211°C, $\nu(N{-}O)$ 1870 cm^{-1}) or similar perchlorate and tetrafluoroborate; a *trans*-structure is indicated by spectroscopic data, and it is presumed to have a linear Ir–N–O grouping.

Unlike Vaska's compound, it does not undergo oxidative addition with O_2, H_2, SO_2 or $(NC)_2C{=}(CN)_2$. (The isoelectronic ruthenium nitrosyl $RuCl(NO)(PPh_3)_2$ likewise binds SO_2 and O_2.) This has been ascribed to the increased positive charge on iridium and also to the nitrosyl group syphoning off π-electron density. The iridium compound will, however, undergo a number of addition reactions with both neutral donors and anionic ligands (Figure 2.102).

These reactions are accompanied by pronounced shifts in the positions of $\nu(N{-}O)$ in the IR spectrum, almost certainly associated with the transition to bent Ir–N–O linkages, known from X-ray data for two of the products.

Comparison of four pairs of compounds where the structures of both rhodium and iridium analogues are known shows dangers of drawing correlations between spectra and structure, even with isoelectronic compounds.

1. $[M(NO)_2(PPh_3)_2]^+$. The coordination number of the metal in both is four, in a distorted tetrahedral geometry. The position of $\nu(N{-}O)$ in the IR spectrum is essentially the same, and the rhodium and iridium compounds have similar slight bending of the M–N–O linkage.

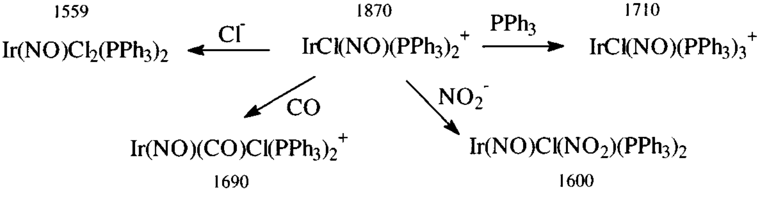

Figure 2.102 Addition reactions for iridium nitrosyl complexes ($\nu(N{-}O)$ (cm^{-1}) is shown for each compound).

2. $M(NO)(PPh_3)_3$. Though the M–N–O bond angles are very different (180° (Ir) and 157° (Rh)), ν(N–O) occurs at virtually the same position in the IR spectrum.
3. $M(NO)Cl_2(PPh_3)_2$. Both these compounds have a square pyramidal structure with bent apical M–N–O linkage and similar bond angles. There is, however, a difference of $70\,cm^{-1}$ in ν(N–O).
4. $M(NO)(OCOCF_3)_2(PPh_3)_2$. Both these complexes have 5-coordinate geometries with monodentate carboxylates. The rhodium compound has a square pyramidal structure with bent Rh–N–O (122°) but the iridium compound has a tbp structure with 'straight' equatorial Ir–N–O (178°). The position of ν(N–O) reflects this difference ($1800\,cm^{-1}$ (Ir) and $1665\,cm^{-1}$ (Rh)).

The balance between linear and bent nitrosyl coordination is delicate, illustrated by the case of the allyl complex $[Ir(NO)(C_3H_5)(PPh_3)_2]^+$. When precipitated as the PF_6^- salt, it exhibits ν(N–O) at $1763\,cm^{-1}$; the BF_4^- salt shows ν(N–O) at $1631\,cm^{-1}$. Solutions of either compound show both bands, with the intensity of the $1763\,cm^{-1}$ band increasing on cooling. NMR shows that the allyl group is present as a π-allyl throughout. The solid-state structure of the BF_4 salt shows a bent nitrosyl (Ir–N–O 129°; X-ray) so that the higher value of ν(N–O) is associated with a straight Ir–N–O linkage; the two isomeric forms are thus in equilibrium in solution (Figure 2.103) [184].

Many of the nitrosyls studied are 5-coordinate, and analysis of crystallographic results indicates that, in general, in the trigonal bipyramid structures NO is found in the equatorial position in a linear geometry whereas in a square pyramidal structure, there is a bent M–N–O linkage in an apical position. A further point of interest is that in compounds like $Ir(NO)Cl_2(PPh_3)_2$, the nitrosyl group bends in the more hindered (P–Ir–P) plane.

Extended-Hückel calculations have been carried out [185] for systems such as $IrCl_4(NO)^{2-}$, based on a slightly distorted square pyramid of C_{4v} symmetry (crystallographically studied 5-coordinate systems do not have a planar base but exhibit this slight distortion). Figure 2.104 shows how the

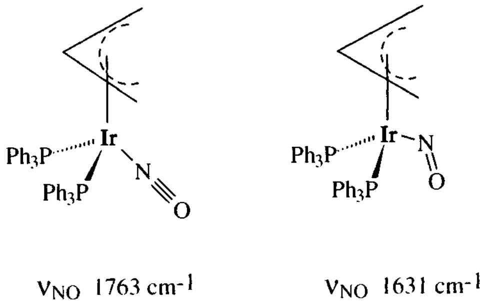

Figure 2.103 Bent and linear allyl nitrosyls.

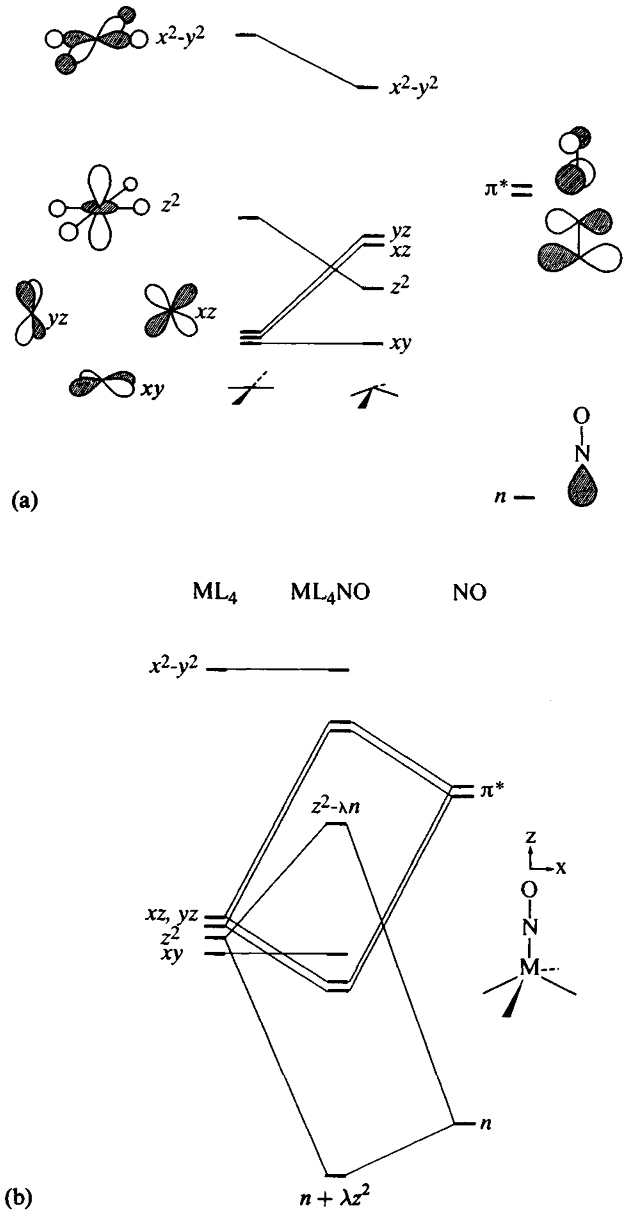

Figure 2.104 (a) Energy levels of (left) square planar and (centre) pyramidally distorted complexes, together with (right) key donor and acceptor orbitals of a nitrosyl ligand. (b) Interaction diagram for a linear nitrosyl in the apical position of a square pyramidal $ML_4(NO)$ system. (Reprinted with permission from *Inorg. Chem.*, 1974, **13**, 2667. Copyright (1974) American Chemical Society.)

metal d orbitals in a C_{4v} MX_4 situation interact with the orbitals of a linear NO; principally this involves d_{z^2} mixing with the lone pair on N (n) and the π-interaction between metal d_{xz}, d_{yz} and the π^* pair of NO orbitals, as shown in Figure 2.104.

In a complex $Ir(NO)Cl_4^{2-}$ or $Ir(NO)Cl_2(PR_3)_2$ there are 10 electrons associated with these levels. A system widely used to represent this situation (developed by Enemark and Feltham) neglects the two electrons in the orbital $(n + \lambda z^2)$ largely derived from the N lone pair, thus describing $Ir(NO)Cl_4^{2-}$ as $\{MNO\}^8$, meaning that there are eight electrons associated with the metal d orbitals and NO π^*-orbitals; this counts the metal and NO together and gets rid of any dichotomy surrounding assignment of the oxidation state of the metal. Thus for $Ir(NO)Cl_4^{2-}$, in Figure 2.104, the MOs are occupied up to and including $z^2 - \lambda n$.

The effect of bending the Ir–N–O linkage in the xz plane is shown in the Walsh diagram (Figure 2.105).

As the Ir–N–O angle decreases below 180°, two interactions change. Firstly, the d_{z^2} interactions with the nitrogen one pair n grows weaker; as Figure 2.105 shows, in a linear case it is destabilizing so that lessening it increases stability. Secondly d_{z^2} begins to form a bonding interaction with π^*_{xz}, while the interactions of d_{xz} with π^* decreases.

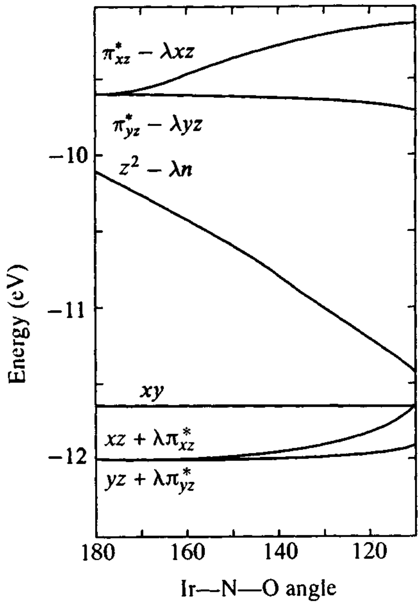

Figure 2.105 Walsh diagram for an $[IrCl_4(NO)]^{2-}$ system. (Reprinted with permission from *Inorg. Chem.*, 1974, **13**, 2667. Copyright (1974) American Chemical Society.)

Reference to the Walsh diagram (Figure 2.105) shows that for a $\{MNO\}^8$ system, bending produces a net stabilization, thus rationalizing the M–N–O bond angle of *c.* 120° found for systems like $M(NO)Cl_2(PR_3)_2$.

The energies of the d_{z^2} and d_{xz} orbitals can also be significantly altered by changing ligands, with strong π-donors increasing the levels of the metal π-orbitals and tending to favour bending.

Calculations for trigonal bipyramidal $ML_4(NO)$ systems with axial NO-like $[Ir(NO)(PPh_3)_3H^+]$ give a d orbital sequence of $xz, yz < x^2 - y^2, xy < z^2$ so that in such an $\{IrNO\}^8$ system, the z^2 orbital is unoccupied; not only does bending not produce any stabilization but in fact d_{xz}, $d_{yz} - \pi^*$ back-bonding is lost, favouring a linear Ir–N–O bond.

2.17 Simple σ-bonded alkyls and aryls of rhodium and iridium

A number of the simple σ-bonded alkyls and aryls of rhodium and iridium have been synthesized in recent years. There are three types of rhodium(III) methyl derivative

$$MCl_3(C_4H_8S)_3 \xrightarrow[\text{Et}_2\text{O, tmed}]{6\text{MeLi}} [Li(tmed)]_3(MMe_6)^{3-} \qquad (M = Rh, Ir)$$

$$\xrightarrow[(M=Rh)]{PMe_3} fac\text{-}RhMe_3(PMe_3)_3$$

The hexamethyl anions are analogous to the series formed by the lanthanides; they have octahedrally coordinated metals (Rh–C 2.13 Å; Ir–C 2.16 Å) but decompose above 20°C. A different compound of the formula $RhMe_3(PMe_3)_3$, possibly the *mer*-isomer, is made from $Rh_2(O_2CMe)_4$ and PMe_3, using $MgMe_2$ as the alkylating agent [186]. Other *fac*-alkyls, Rh(alkyl)(1,4,7-trialkyl-1,4,7-triazacyclononame) compounds have been made (alkyl = Me, neohexyl) [187].

Aryls have recently been synthesized [188], including a rare rhodium(II) compound (Figure 2.106).

The rhodium(III) triaryls have pseudo-octahedral structures; therefore, in the air-stable trimesityl rhodium, the three mesityl groups are arranged in *fac*-positions, with *ortho*-methyls blocking the other coordination sites (Figure 2.107).

Trimesityl rhodium is reduced by PMe_2Ph to give a square planar rhodium(I) aryl

$$Rh(2,4,6\text{-}Me_3C_6H_2)_3 \xrightarrow{PMe_2Ph} Rh(2,4,6\text{-}Me_3C_6H_2)(PMe_2Ph)_3$$

Anhydrous $IrCl_3$ reacts with excess mesityllithium to form air-stable tetramesityliridium, which has a distorted tetrahedral structure; as expected

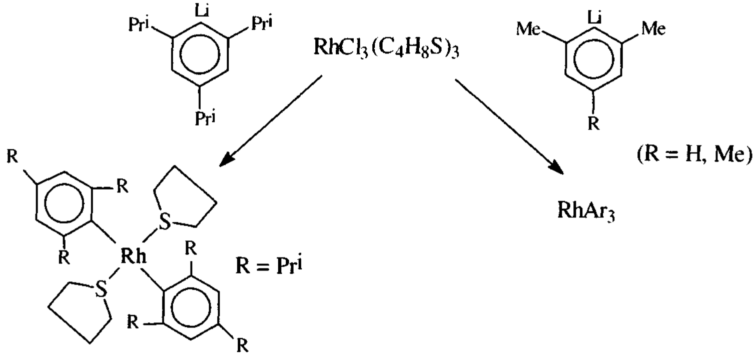

Figure 2.106 Synthesis of rhodium aryls.

for iridium(IV), low spin d^5, it gives an ESR signal ($g_\perp = 2.005$; $g_{\parallel} = 2.437$) [189].

The trimesityl of iridium can be made by reaction of $IrCl_3(tht)_3$ with MesMgBr, while $IrMes_4$ can be oxidized to the cationic iridium(V) species $[IrMes_4]^+$, also tetrahedral (with concomitant slight Ir—C bond changes from 1.99–2.04 Å in the neutral compound to 2.004–2.037 Å in the cation). Another iridium(V) species, $IrO(Mes)_3$ has been made [190], it has a tetrahedral structure (Ir=O 1.725 Å).

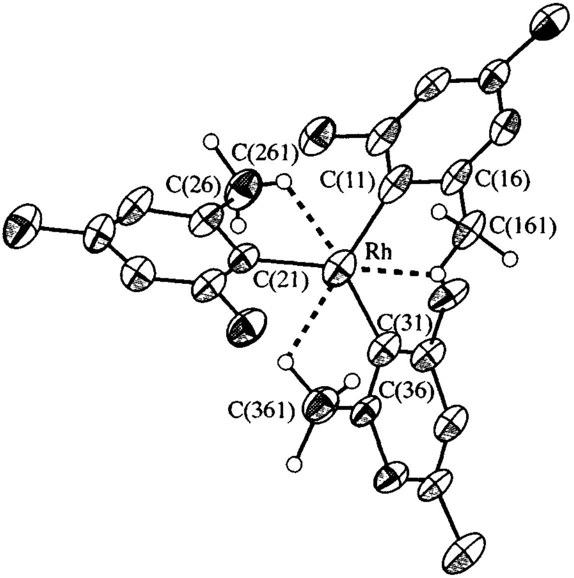

Figure 2.107 The structure of trimesitylrhodium. (Reproduced with permission from *J. Chem. Soc., Chem. Commun.*, 1990, 1242.)

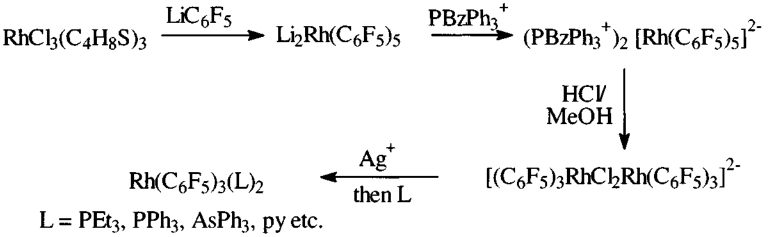

Figure 2.108 Synthesis of rhodium pentafluophenyl complexes.

Reaction of an 'aberrant batch' of $IrCl_3.xH_2O$ with mesityllithium has given a substituted hexadienyl rather than $IrMes_4$ [191].

Using the electron-withdrawing pentafluorophenyl group, two types of 5-coordinate compound have been made (Figure 2.108).

The anionic pentafluorophenyls have square pyramidal structures but are evidently non-rigid in solution (^{19}F NMR shows all ligands equivalent). The neutral adducts are also square pyramidal (apical C_6F_5, *trans*-L) [192].